

Nanosphere Arrays with Controlled Sub-10-nm Gaps as Surface-Enhanced Raman Spectroscopy Substrates

Hui Wang, Carly S. Levin, and Naomi J. Halas*

Department of Chemistry and Department of Electrical and Computer Engineering, Rice University, Houston, Texas 77005

Received August 17, 2005; E-mail: halas@rice.edu

Since its initial discovery, surface-enhanced Raman scattering (SERS) has exhibited extraordinary potential for the characterization of trace chemical species.¹ One highly promising approach for the design of SERS substrates involves the positioning or fabrication of nearly adjacent metallic nanostructures with nanoscale gaps. Gaps between adjacent metallic nanostructures have been shown to support extremely intense local electromagnetic fields, known as “hot spots”, upon optical excitation.^{2,3} It is essentially these features that have been attributed to the enormous SERS enhancements reported for random colloidal aggregates, approaching single-molecule sensitivity for certain molecules.^{4,5}

The precise properties and geometric requirements for nanoscale junctions and their plasmon excitations have been the subject of detailed theoretical studies since the early 1980s.⁶ A recent model for the junction excitations of metallic nanostructures, known as plasmon hybridization, draws a direct analogy between the plasmon excitations of a pair of directly adjacent metallic nanostructures and the excited states of simple homonuclear diatomic molecules.^{7,8} In this picture, the plasmon excitations of two adjacent metallic nanoparticles hybridize to form two “dimer” plasmons, where the low-energy “bonding” plasmon is responsible for the high optical intensity in the nanoscale interparticle junctions. In these studies it was shown that the interparticle spacings required to achieve large SERS enhancements in a junction geometry are in the sub-10-nm range. While junctions in this size range have likely been experimentally achieved in random colloidal aggregates and fractal films, the controlled fabrication of highly regular, metallic nanostructure geometries with a high density of sub-10-nm interparticle spacings is beyond current nanofabrication methods.^{9,10}

Here we describe a convenient and cost-effective chemical approach to fabricating highly ordered Au spherical nanoparticle (NP) arrays with sub-10-nm spacing between adjacent nanoparticles, which exhibit high, stable, and reproducible SERS activity. Figure 1A schematically illustrates the fabrication procedure for Au nanosphere arrays. Au nanospheres of 50 nm in diameter were functionalized with cetyltrimethylammonium bromide (CTAB) and then redispersed in water to form colloidal solutions ($\sim 10^{12}$ particles mL^{-1}). Drying a 10- μL droplet of CTAB-capped Au colloid solution on indium-doped tin oxide (ITO) glass under ambient conditions resulted in the formation of hexagonally close-packed monolayer NP arrays with average interparticle distance of ~ 8 nm. The interparticle spacing was determined from SEM images (Figure 1B) and is consistent with the reported ~ 2.2 -nm thickness of a single CTAB layer. As a capping surfactant, CTAB can form self-assembled bilayers on Au nanostructures. The bilayer capping of CTAB on Au NPs leads to a net positive charge on the NP surfaces, providing a net repulsive interaction between the NPs to prevent random disordered aggregation during solvent evaporation.^{11,12}

As shown in Figure 1D, the as-fabricated NP arrays display a broad and intense plasmon band in the near-infrared region. This

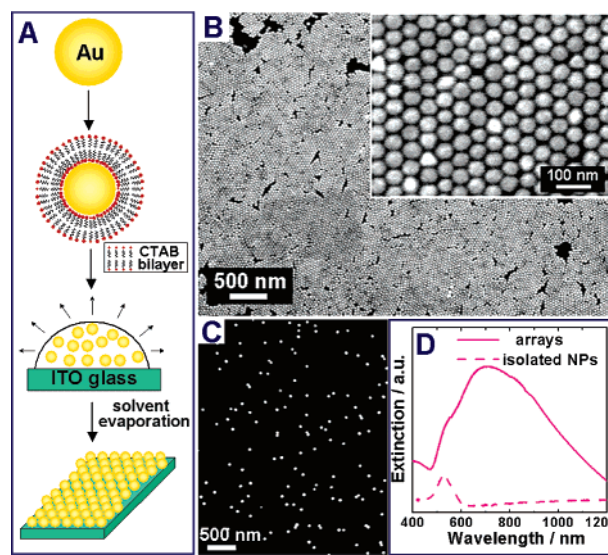


Figure 1. (A) Schematic illustration of the fabrication of sub-10-nm gap Au NP arrays. (B) SEM image of the arrays. (C) SEM image of monolayer of isolated Au NPs on ITO glass. (D) Vis-NIR extinction spectrum of the monolayer of isolated Au NPs and arrays.

band arises from a coalescence of the dimer plasmon resonances of the individual junctions^{7,13} in the array to form a band, in analogy with electronic energy bands in solids and pass bands in photonic crystals. When illuminated in this absorption band, the NP arrays exhibit enormous near-field enhancements at the junctions between neighboring NPs, creating uniform densities of well-defined “hot spots” exploitable for large SERS enhancements. Using periodic nanostructured SERS substrates like this can provide detailed and quantitative correlations between surface structures and SERS enhancements.^{14–17} From the electromagnetic point of view, these NP arrays can be regarded as “inverse Van Dyne lattices”, possessing near-field properties similar but complementary to those of the triangle arrays fabricated using nanosphere lithography.^{15,16}

The SERS performance of the arrays is quantitatively evaluated using a nonresonant molecule, *p*-mercaptoaniline (pMA), as the analyte. pMA is ideal for quantification because it forms self-assembled monolayers (SAMs) with a known packing density on Au surfaces.¹⁸ pMA can displace CTAB on Au surfaces due to the stronger Au–S bond relative to Au–Br. Figure 2 shows the SERS spectra of pMA for a range of pMA concentrations adsorbed on the NP arrays. The SERS spectra of pMA on the NP arrays are reproducible at different sites on a substrate, with a standard deviation of $<12\%$. As the concentration of pMA increases, the SERS Stokes intensities corresponding to the Au–Br (190 cm^{-1}) and C–C (1045 cm^{-1}) bonds of CTAB progressively decrease, while those of the Au–S (390 cm^{-1}) and C–C bonds of pMA (1005 , 1077 , 1179 , and 1590 cm^{-1}) increase, indicating the gradual

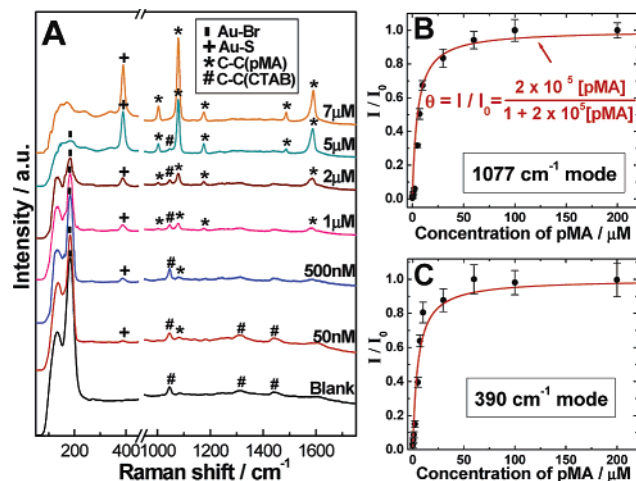


Figure 2. (A) SERS spectra of 5 μL of pMA with different concentrations deposited on the NP arrays. The excitation laser wavelength is 785 nm. Adsorption isotherm of pMA on the NP arrays obtained according to (B) 1077 and (C) 390 cm^{-1} modes in the SERS spectra. I_0 is the peak intensity of a saturated pMA monolayer.

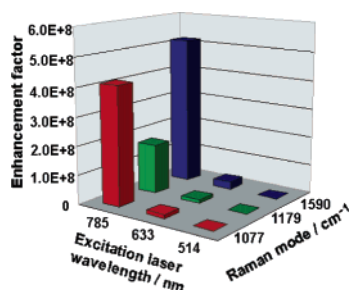


Figure 3. Empirical SERS enhancement factors obtained on the basis of different Raman modes under different laser excitations.

displacement of CTAB by pMA. The Stokes intensities of pMA follow a Langmuir isotherm (Figure 2B,C). A saturated monolayer adsorption of pMA is reached when the concentration of pMA is $> 50 \mu\text{M}$. It is important to note that the displacement of CTAB by the much smaller pMA layer does not affect interparticle spacing of the arrays. The array plasmon maximum shifts from ~ 730 to ~ 785 nm upon CTAB displacement, due to the increased refractive index of pMA.

Empirical enhancement factors were calculated by comparing ratios of the SERS peak intensity of saturated pMA coverage to the corresponding unenhanced signals from neat pMA films of known thickness (0.5 mm). Figure 3 shows the enhancement factors as a function of excitation wavelength. Larger SERS enhancements are observed when the laser wavelength approaches the maximum of the broad array plasmon feature. Empirical enhancement factors above 1×10^8 are observed under near-infrared (785 nm) excitation. This is in precise agreement with the previously reported theoretical prediction for averaged SERS enhancements on Au nanosphere arrays of similar geometry.¹³ This value averages over the entire array surface area: the localized enhancement for the molecules in the interparticle junctions is anticipated to be several orders of magnitude higher.^{17,19,20} Theoretical estimates of the local enhancement in the junctions of this geometry for nonresonant molecules are on the order of 10^{11} or higher.²¹

The arrays can also be used for SERS of dye molecules, such as Rhodamine 6G, Crystal Violet, and Indocyanine Green. The dye molecules appear to intercalate into the CTAB bilayers in the regions where large SERS enhancements arise.

In contrast to many conventional SERS substrates whose SERS activity can be easily compromised,²² our NP arrays display quite stable SERS enhancements. There is no observable activity loss within 30 days, and after 90 days SERS enhancements are reduced by 50% relative to measurements performed on freshly prepared array substrates.

In conclusion, highly ordered NP arrays with sub-10-nm gaps have been fabricated through self-assembly of CTAB-capped Au NPs and have been used as SERS substrates which exhibit high SERS activity, stability, and reproducibility. The displacement of CTAB by thiolated molecules such as pMA, *p*-mercaptobenzoic acid, and cysteine results in the formation of amine or carboxyl moiety terminated SAM capping layers for these substrates, which can potentially serve as cross-linking agents for attachment and SERS-based recognition of nonthiolated molecules. A detailed study using the NP arrays as SERS substrates for biomolecular sensing is currently underway.

Acknowledgment. We gratefully acknowledge NSF (EEC-0304097), AFOSR (F49620-03-C-0068), the Robert A. Welch Foundation (C-1220), and MURI (W911NF-04-01-0203) for their financial support.

Supporting Information Available: Experimental details, extinction spectra of the arrays capped with pMA SAMs, SERS of pMA SAMs on the arrays under different laser excitations, stability of SERS activity of the arrays, and SERS of dyes on the arrays. This information is available free of charge via the Internet at <http://pubs.acs.org>.

References

- (1) Jeanmaire, D. L.; Van Duyne, R. P. *J. Electroanal. Chem.* **1977**, *84*, 1–20.
- (2) Gunnarsson, L.; Rindzevicius, T.; Prikulis, J.; Kasemo, B.; Kall, M.; Zou, S. L.; Schatz, G. C. *J. Phys. Chem. B* **2005**, *109*, 1079–1087.
- (3) Schuck, P. J.; Fromm, D. P.; Sundaramurthy, A.; Kino, G. S.; Moerner, W. E. *Phys. Rev. Lett.* **2005**, *94*, 017402.
- (4) Kneipp, K.; Wang, Y.; Kneipp, H.; Perelman, L. T.; Itzkan, I.; Dasari, R. R.; Feld, M. S. *Phys. Rev. Lett.* **1997**, *78*, 1667–1670.
- (5) Nie, S.; Emory, S. R. *Science* **1997**, *275*, 1102–1106.
- (6) Aravind, P. K.; Nitzan, A.; Metiu, H. *Surf. Sci.* **1981**, *110*, 189–204.
- (7) Nordlander, P.; Oubre, C.; Prodan, E.; Li, K.; Stockman, M. I. *Nano Lett.* **2004**, *4*, 899–903.
- (8) Brandl, D. W.; Oubre, C.; Nordlander, P. *J. Chem. Phys.* **2005**, *123*, 024701.
- (9) Hatzor, A.; Weiss, P. S. *Science* **2001**, *291*, 1019–1020.
- (10) Qin, L. D.; Park, S.; Huang, L.; Mirkin, C. A. *Science* **2005**, *309*, 113–115.
- (11) Nikoobakht, B.; Wang, Z. L.; El-Sayed, M. A. *J. Phys. Chem. B* **2000**, *104*, 8635–8640.
- (12) Orendorff, C. J.; Hankins, P. L.; Murphy, C. J. *Langmuir* **2005**, *21*, 2022–2026.
- (13) Genov, D. A.; Sarychev, A. K.; Shalaev, V. M.; Wei, A. *Nano Lett.* **2004**, *4*, 153–158.
- (14) Tessier, P. M.; Velev, O. D.; Kalambur, A. T.; Rabolt, J. F.; Lenhoff, A. M.; Kaler, E. W. *J. Am. Chem. Soc.* **2000**, *122*, 9554–9555.
- (15) Haynes, C. L.; Van Duyne, R. P. *J. Phys. Chem. B* **2003**, *107*, 7426–7433.
- (16) McFarland, A. D.; Young, M. A.; Dieringer, J. A.; Van Duyne, R. P. *J. Phys. Chem. B* **2005**, *109*, 11279–11285.
- (17) Wei, A.; Kim, B.; Sadler, B.; Tripp, S. L. *ChemPhysChem* **2001**, *2*, 743–745.
- (18) Mohri, N.; Matsushita, S.; Inoue, M.; Yoshikawa, K. *Langmuir* **1998**, *14*, 2343–2347.
- (19) Garcia-Vidal, F. J.; Pendry, J. B. *Phys. Rev. Lett.* **1996**, *77*, 1163–1166.
- (20) Xu, H. X.; Bjerneld, E. J.; Kall, M.; Borjesson, L. *Phys. Rev. Lett.* **1999**, *83*, 4357–4360.
- (21) Xu, H. X.; Aizpurua, J.; Kall, M.; Apell, P. *Phys. Rev. E* **2000**, *62*, 4318–4324.
- (22) Norrod, K. L.; Sudnik, L. M.; Rousell, D.; Rowlen, K. L. *Appl. Spectrosc.* **1997**, *51*, 994–1001.

JA055633Y